
It’s All Connected: Topology-Aware Structural Graph Encoding Improves Performance on Polymer Prediction

Halil I. Erdogan¹, Punith Raviswamy¹, Nikita Agrawal², Yannik Köster^{3,4},
Stefan Zechel^{3,4,5,6}, Ulrich S. Schubert^{3,4,5,6}, Ruben Mayer², Christopher Kuenneth¹✉,

¹Faculty of Engineering Science, University of Bayreuth, Germany

²Faculty of Mathematics, Physics & Computer Science, University of Bayreuth, Germany

³Laboratory of Organic and Macromolecular Chemistry (IOMC), Friedrich Schiller University Jena, Germany

⁴Jena Center for Soft Matter (JCSM), Friedrich Schiller University Jena, Germany

⁵Helmholtz Institute for Polymers in Energy Applications Jena (HIPOLE Jena), Germany

⁶Helmholtz Zentrum Berlin für Materialien und Energie GmbH (HZB), Germany

✉ Corresponding author: christopher.kuenneth@uni-bayreuth.de

Abstract

Graph Neural Networks (GNNs) have achieved strong results in molecular property prediction, but polymers present distinct challenges: labeled datasets are scarce and small (typically in the order of hundreds of polymers) due to the need for expensive experimentation, and complex polymer chain distributions influence polymer properties. Established practice in polymer prediction represents polymers solely by graphs of their repeat units, discarding the chain-scale morphology that governs key properties such as the glass transition temperature (T_g). In this work, we propose a principled graph construction that addresses this gap. Given a polymer’s molar mass distribution (MMD), we sample representative chains from the Schulz-Zimm distribution and construct representative sets of large graphs encoding chain-scale topology directly, with atoms and bonds featurized using rich chemical descriptors. We further pretrain GNN encoders via masked graph modeling on 100,000 unlabeled PSMILES strings before fine-tuning on labeled data. On a dataset of 381 polymers (180 homopolymers and 201 copolymers), we show that graph construction and self-supervised pretraining are jointly necessary: without pretraining, the large graph method matches the repeat-unit baseline (28.40 K vs. 28.36 K RMSE); with pretraining, it achieves $24.76 \text{ K} \pm 3.30 \text{ K}$, a 5.1% reduction in mean error over the pretrained repeat-unit baseline ($26.08 \text{ K} \pm 4.20 \text{ K}$, $p < 0.001$, 30 runs). An ablation removing chemical features degrades performance to 36.65 K, confirming both components are essential. Results are architecture-agnostic, holding for both GINE and GATv2 encoders.

1 Introduction

Machine learning (ML), particularly neural networks, has accelerated polymer discovery and design by predicting properties from chemical structures [1, 2]. Polymer informatics [3], a burgeoning field at the intersection between ML and materials science, focuses on polymers ubiquitous in plastics, coatings, and electronics, targeting thermal, mechanical, and electronic properties. One prominent polymer property is glass transition temperature (T_g) measured in Kelvin (K): the temperature where polymers shift from rigid (glassy) to flexible (rubbery) states, dictating mechanical performance under thermal stress [4]. Graph Neural Networks (GNNs) perform well in this setting by modeling polymers as graphs (atoms as nodes, and bonds as edges), with prior successes in using repeat units (monomeric building blocks) directly as the graph encoding [5, 6]. However, this approach omits the

inherent complexity of polymer chain topologies, specifically the molar mass distribution (MMD). This distribution, defined by the number-average molar mass (M_n), weight-average molar mass (M_w), and dispersity (\mathfrak{D}), profoundly impacts bulk macroscopic properties, including T_g , as e.g., postulated by the Fox-Flory relation [7, 8].

Standard GNNs are formulated as deterministic functions mapping a single graph G to a target y , i.e., $f(G) = y$. In contrast, polymer systems are more naturally described as distributions over graphs induced by chain length variability. As a result, the prediction task is better viewed as learning a function over graph distributions, i.e., approximating $\mathbb{E}_{G \sim \mathcal{D}}[f(G)] \approx y$, where \mathcal{D} represents the chain length distribution. This is particularly challenging for polymers. Repeating units form theoretically endless chains of diverse lengths, making exhaustive graph encodings impractical. MMD profiles describe ensembles of chains rather than discrete structures, while branching in copolymers resists canonical graph encoding approaches. Limited experimental data further constrains representation optimization. Sophisticated augmentations beyond basic repeat-unit graphs are therefore mission-critical [5, 6].

We address these challenges through two complementary contributions. First, we propose representing each polymer as sets of large graphs whose chain lengths are sampled from the Schulz-Zimm molar mass distribution [9]. Given M_n , M_w , and \mathfrak{D} , we parameterize a Gamma distribution and draw multiple independent sets of chains, constructing a graph that encodes the distributional shape of chain lengths directly into the topology accessible to the GNN. Each polymer is described by a polymer SMILES (PSMILES) string [10], an extension of the Simplified Molecular Input Line Entry System (SMILES) representation [11], and each atom and bond in the sampled chains is encoded with rich chemical features computed via RDKit [12], including atom type, hybridization, chirality, degree, and bond order, providing the GNN with the chemical identity it needs alongside the structural context. Second, we pretrain GNN encoders via masked graph modeling on 100,000 unlabeled PSMILES strings, giving the encoder a structural and chemical vocabulary before any labeled T_g data is seen. We show that these components are mutually necessary: without pretraining, the large graphs offer no advantage over a repeat-unit graph; with pretraining, the structural encoding yields a statistically significant improvement.

Our main contributions are:

- A principled large-graph construction for polymer property prediction based on Schulz-Zimm MMD sampling [9], embedding chain-scale structure directly into graph topology rather than as decoder-level scalars. This is the basis for our Monte Carlo approximation of the T_g expectation for polymer systems.
- Rich chemical node and edge feature encoding via RDKit [12], shown by ablation to be essential: a topology-only graph without chemical features yields 36.65 K RMSE, an 11.89 K degradation relative to the full model.
- An empirical analysis demonstrating that graph construction and self-supervised pretraining are jointly necessary: large graphs without self-supervised pretraining (SSL) match repeat-unit graphs, while the combination achieves $24.76 \text{ K} \pm 3.30 \text{ K}$ RMSE vs. $26.08 \text{ K} \pm 4.20 \text{ K}$ for the repeat-unit baseline ($p < 0.001$, paired t -test, 30 runs).
- Architecture-agnostic results across GINE [13] and GATv2 [14] encoders, confirming the gain originates from the graph construction and pretraining strategy rather than model-specific inductive biases.
- Uncertainty quantification via Monte Carlo Dropout [15], providing per-polymer predictive uncertainty estimates alongside point predictions.

2 Background

Graph Neural Networks. GNNs operate on graphs by iteratively aggregating information from local neighbourhoods via message passing [16, 17]. At each layer ℓ , a node v updates its representation by aggregating messages from its neighbours $\mathcal{N}(v)$:

$$\mathbf{h}_v^{(\ell+1)} = \text{UPDATE} \left(\mathbf{h}_v^{(\ell)}, \text{AGGREGATE} \left(\{(\mathbf{h}_u^{(\ell)}, \mathbf{e}_{uv}) : u \in \mathcal{N}(v)\} \right) \right) \quad (1)$$

where \mathbf{e}_{uv} are edge features. After L layers, a global readout (e.g. mean pooling) produces a graph-level embedding, which is passed to a multi-layer perceptron (MLP) for prediction. We evaluate two

message-passing variants: GINE [13], which incorporates edge features into the aggregation via a sum-based update, and GATv2 [14], which uses dynamic attention coefficients to weight neighbour contributions.

Self-supervised pretraining. Self-supervised learning (SSL) on graphs trains an encoder without labels by solving auxiliary tasks defined on the graph structure itself. We use masked graph modeling, where a fraction of node and edge features are masked and the model is trained to reconstruct them [13]. Pretraining on large unlabeled corpora provides the encoder a general structural vocabulary that can be transferred to downstream tasks with limited labeled data.

Polymer chains and molar mass distributions. Polymer chains are macromolecules made by polymerizing many small monomer molecules into long chains. Depending on the monomer units’ functionality and reaction pathway, polymerization generates e.g., linear chains, branched, or network structures. When two or more different monomer molecule types are present, the macroscopic structure is called a copolymer with varying distributions of monomers.

Polymers or polymer materials are not just single chains but distributions of chain lengths and architectures, quantified by molar mass statistics: M_n (number-average molar mass), M_w (weight-average molar mass), and $\mathfrak{D} = M_w/M_n$ (dispersity of chain lengths) [9]. A \mathfrak{D} of 1 indicates perfectly uniform chains (monodisperse, rare in practice), while $\mathfrak{D} > 2$ is typical for industrial polymers, reflecting broad chain length variation within one sample. This structural polydispersity makes polymers far more complex than small molecules, as identical repeat units can yield vastly different chain configurations and bulk properties, and consequently makes it more challenging for GNNs to learn consistent representations.

Higher M_n increases chain entanglement, enhancing mechanical strength but raising processing viscosity. The glass transition temperature (T_g), a reversible transition from rigid/glassy to flexible/rubbery states, is particularly sensitive to MMD, rising with molar mass [9]. \mathfrak{D} broadens the distribution of T_g within samples. These ensemble effects fundamentally distinguish polymers from discrete small molecules, creating unique challenges for computational property prediction.

3 Problem Formulation

We consider the problem of predicting a scalar polymer property (specifically the glass transition temperature $T_g \in \mathbb{R}$) from the chemical structure of a polymer and associated molecular descriptors. We introduce notation used throughout the paper.

Polymer representation. A polymer is described by its PSMILES string [10], an extension of the standard SMILES notation [11] in which two dummy atoms ($[*]$) mark the polymerization attachment sites of the repeat unit. We consider two classes of polymers: homopolymers, characterized by a single repeat unit with PSMILES s , where the chain is formed by repeating s for n repetitions connected at the attachment sites (n being the degree of polymerization determined by the molar mass distribution); and copolymers, characterized by two distinct repeat units with PSMILES s_1 and s_2 combined in molar fractions $\phi_1, \phi_2 \in [0, 1]$ with $\phi_1 + \phi_2 = 1$. As our dataset contains only polymers with two monomer types, we consider binary copolymers corresponding to random copolymers, where repeat units are distributed randomly along the backbone according to their relative composition.

In addition to the PSMILES string, each polymer is associated with a vector of global molecular descriptors. For homopolymers, $\mathbf{g} = (M_n, M_w, \mathfrak{D}, M_0) \in \mathbb{R}^4$, where M_n is the number-average molar mass, M_w is the weight-average molar mass, $\mathfrak{D} = M_w/M_n$ is the dispersity, and M_0 is the repeat-unit molar mass. For copolymers, the descriptor is extended to $\mathbf{g} = (M_n, M_w, \mathfrak{D}, M_0, \phi_1, \phi_2) \in \mathbb{R}^6$. For homopolymers, we set $(\phi_1, \phi_2) = (1, 0)$, so all polymers share a uniform 6-dimensional input to the decoder.

Graph representation. We represent a polymer as a graph $\mathcal{G} = (\mathcal{V}, \mathcal{E}, \mathbf{X}, \mathbf{E})$, where \mathcal{V} is the set of nodes (atoms), $\mathcal{E} \subseteq \mathcal{V} \times \mathcal{V}$ is the set of edges (bonds), treated as undirected, $\mathbf{X} \in \mathbb{R}^{|\mathcal{V}| \times d_v}$ is the node feature matrix with d_v -dimensional atom features per node, and $\mathbf{E} \in \mathbb{R}^{|\mathcal{E}| \times d_e}$ is the edge feature matrix with d_e -dimensional bond features per edge. The specific choice of node and edge feature

encodings, together with the graph topology (i.e., which atoms and bonds are included), constitute the *graph construction* and are the central focus of this work.

Task. Given a dataset $\mathcal{D} = \{(\mathcal{G}_i, \mathbf{g}_i, T_{g,i})\}_{i=1}^N$ of N labeled polymers, the goal is to learn a function

$$f : (\mathcal{G}, \mathbf{g}) \longrightarrow \hat{T}_g \in \mathbb{R} \quad (2)$$

that minimizes the mean squared error $\frac{1}{N} \sum_{i=1}^N (\hat{T}_{g,i} - T_{g,i})^2$ over the dataset.

Key question. The central challenge is not the choice of GNN architecture for f , but rather the *graph construction*: given a PSMILES string, how should \mathcal{G} be defined such that the resulting representation is highly informative for property prediction? Unlike small molecules, polymers are macromolecules with no single well-defined molecular graph. The repeat unit captures only local chemical identity, while chain-scale structures, such as chain topology distributions and monomer sequences, critically determine macroscopic properties such as T_g . This tension between local chemistry and chain-scale physics and chemistry is the core difficulty in polymer graph construction, and it is the problem we address in this work.

4 Why Standard Graph Constructions Fall Short

Scalar descriptors alone are insufficient for GNN embeddings. The dominant approach in GNN-based polymer property prediction is to represent a polymer by the graph of its repeat unit [10, 3]. In this construction, nodes correspond to atoms within a single repeat unit and edges correspond to bonds, with polymerization attachment sites removed. Global molecular descriptors such as M_n , M_w , and \mathfrak{D} are typically appended as scalar features at the graph readout stage. This approach is computationally convenient but introduces a fundamental representational bottleneck. Appending M_n , M_w , and \mathfrak{D} as scalars to the decoder can shift the final prediction globally, but it cannot alter the GNN embeddings produced by message passing. The message-passing layers operate solely on the repeat-unit graph and therefore produce identical node embeddings for all polymers that share the same repeat unit, regardless of how different their chain lengths or molecular weight distributions are. Since T_g and other polymer properties are governed by chain-scale physics (chain length, entanglement density, free volume) that emerge only from the collective arrangement of many repeat units [9], this means the GNN is asked to predict a chain-scale property from a graph that contains no chain-scale information. The scalar descriptors are incorporated too late in the pipeline to compensate. They reach the decoder after the structural embedding is already fixed. Recent work [18] addresses this by using coarse-grained monomer-level graphs with kinetic Monte Carlo-generated chain ensembles; our approach differs in operating at the atom level with full bond-feature encoding and self-supervised pretraining.

Empirical evidence. We confirm this limitation experimentally. Despite both models receiving identical scalar descriptors (M_n , M_w , \mathfrak{D} , M_0), the repeat-unit construction underperforms our proposed approach when both are combined with self-supervised pretraining, which encodes the molar mass distribution directly into the graph topology. The improvement is statistically significant ($p < 0.001$, paired t -test) and holds across two distinct GNN architectures. Full experimental details and results are reported in Section 7.

5 Proposed Graph Construction

We propose representing a polymer not as a single repeat-unit graph but as an ensemble of full polymer chains whose lengths are sampled from the molar mass distribution of the sample. This embeds chain-scale structure, physically determined by M_n , M_w , and \mathfrak{D} , directly into the graph topology, making it accessible to the GNN’s message-passing layers rather than available only as global scalars at the decoder (Figure 1).

Step 1: Parameterizing the molar mass distribution. Real polymer samples follow a broad distribution of chain lengths described by the Schulz-Zimm distribution [9], which can be expressed as a Gamma distribution. Given M_n , M_w , and monomer mass M_0 , we compute the number-average

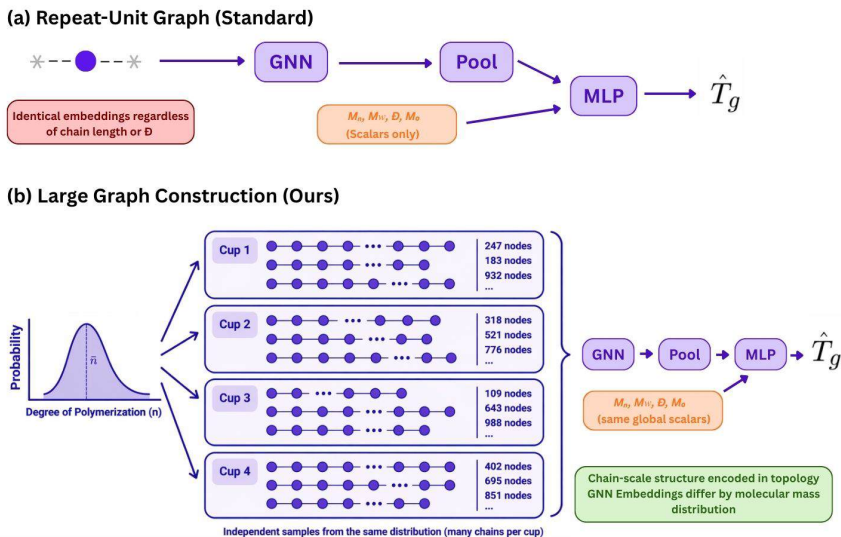


Figure 1: Comparison of graph construction strategies. **(a)** The standard repeat-unit graph produces identical node embeddings for identical repeat-unit graphs, regardless of chain length or \mathfrak{D} ; molar mass information enters only as global scalars. **(b)** Our large-graph construction samples chain lengths from the Schulz-Zimm (Gamma) distribution, embedding chain-scale structure directly into the graph topology accessible to message-passing layers.

degree of polymerization $DP_n = M_n/M_0$ and the dispersity $\mathfrak{D} = M_w/M_n$, and parameterize Gamma(k, θ) as:

$$k = \frac{1}{\mathfrak{D} - 1}, \quad \theta = \frac{DP_n}{k}. \quad (3)$$

To avoid computationally intractable chains, we rescale θ by a factor $\min(1, DP_{\max}/F_{\text{Gamma}}^{-1}(0.99; k, \theta))$, which caps the 99th-percentile DP at $DP_{\max} = 1000$ while preserving the shape parameter k and therefore the qualitative form of the distribution.

Step 2: Sampling chains (cups). For each polymer we generate $C = 4$ independent stratified samples from the parameterized distribution, which we call *cups* (independent sampled graph instances). Each cup contains approximately 30 chains whose DPs are drawn via stratified inverse-CDF sampling over 8 equal-probability quantile bins of the distribution. This can be viewed as a stratified Monte Carlo sampling scheme, providing balanced coverage across both short- and long-chain regimes. Multiple cups per polymer serve as structural replicas, capturing the stochastic variability of the molar mass distribution.

Step 3: Building chain graphs and feature encoding. Each chain of DP n is constructed by extracting the repeat unit from the PSMILES string [10] (removing the two dummy attachment atoms), repeating it n times and connecting adjacent units via explicit bonds at the attachment sites. All chains within a cup are concatenated into a single (disconnected) graph \mathcal{G} , where each chain forms a separate connected component. A GNN with global mean pooling then produces a single polymer embedding from the full multi-chain graph, integrating information across all sampled chain lengths. Each atom is encoded as a $d_v = 31$ -dimensional feature vector comprising: atom type (12 classes), hybridization (4), chirality (3), degree (number of bonds, 7), aromaticity, ring membership, hydrogen count, formal charge, and normalized atomic mass. Each bond is encoded as a $d_e = 14$ -dimensional vector comprising: bond type (5 classes), conjugation, ring membership, and stereochemistry (7). All features are computed with the cheminformatics tool RDKit [12].

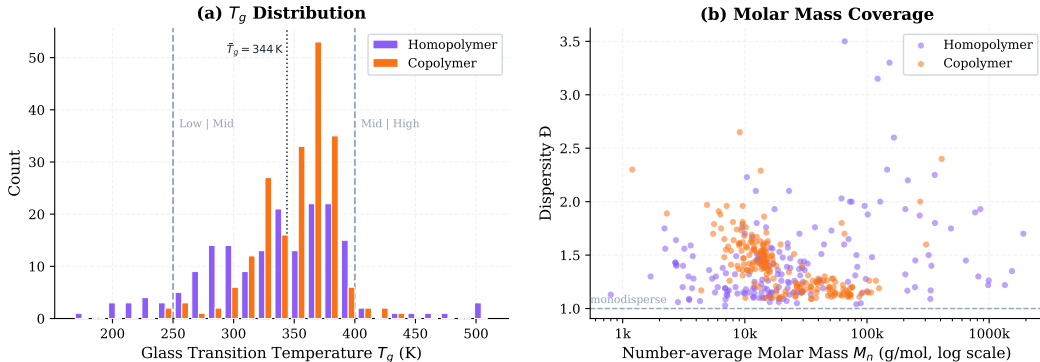


Figure 2: Dataset statistics for the 381-polymer labeled set. **Left:** Distribution of experimentally measured T_g values for homopolymers (purple) and copolymers (orange), with stratum boundaries at 250 K and 400 K indicated by dashed lines. **Right:** Number-average molar mass M_n vs. dispersity \mathfrak{D} (log scale), illustrating the wide range of molar mass distributions present in the dataset.

Copolymers. For copolymers with two repeat units s_1, s_2 and molar fractions ϕ_1, ϕ_2 , the effective monomer mass is $M_0^{\text{eff}} = \phi_1 M_{0,1} + \phi_2 M_{0,2}$, which is used in place of M_0 in Equation 3. Each chain position is assigned repeat unit s_1 or s_2 independently with probabilities ϕ_1 and ϕ_2 , yielding a statistical copolymer sequence consistent with the experimentally measured composition.

Global features. In addition to the graph, we pass the scalar descriptors $\mathbf{g} = (M_n, M_w, \mathfrak{D}, M_0)$ directly to the decoder after global mean pooling. These scalars complement the structural encoding: The graph topology encodes the distributional shape of chain lengths as structural patterns that the GNN can learn through pretraining, while the scalars provide the decoder with precise numerical values of the same quantities.

6 Experimental Setup

Labeled dataset. Polymer records, each comprising repeat-unit chemical identity, molar mass descriptors (M_n, M_w, \mathfrak{D}), and an experimentally measured T_g , were compiled from two polymer reference handbooks [19, 20], the PHA copolymer dataset of Jiang et al. [21], and experimental data contributed by co-authors at Friedrich Schiller University Jena (Y. Köster, S. Zechel, U. S. Schubert). The labeled dataset comprises 381 polymer samples (180 homopolymers and 201 copolymers) with experimentally measured glass transition temperatures spanning $T_g \in [173 \text{ K}, 506 \text{ K}]$ (mean $344 \text{ K} \pm 46 \text{ K}$). Molar mass descriptors cover a wide range: $M_n \in [800 \text{ g mol}^{-1}, 1.905882 \times 10^6 \text{ g mol}^{-1}]$ (median 16 500), $\mathfrak{D} \in [1.0, 3.5]$ (mean 1.4), and $M_0 \in [28 \text{ g mol}^{-1}, 462 \text{ g mol}^{-1}]$. The broad span of M_n and \mathfrak{D} values motivates the use of a distribution-aware graph construction rather than fixed scalar descriptors. Each polymer is represented by $C = 4$ independent sampling instances (“cups”), yielding 1,524 graphs in total. Dataset statistics are visualized in Figure 2. For self-supervised pretraining we sample 100,000 PSMILES [10] strings from the polyOne dataset [22], which contains hypothetical polymers generated by fragment-based combinatorial composition. All strings are chemically valid as ensured by the dataset construction but largely unsynthesized (i.e., without experimental T_g labels), providing a diverse pretraining signal without requiring experimental labels.

Models. We evaluate two GNN architectures to demonstrate that our graph construction generalizes across architectures. Both share the same encoder design: 3 message-passing layers with hidden dimension 32, GraphNorm [23], GELU activations, residual connections, and dropout ($p = 0.1$). The two variants are:

- **GINE** [13]: Graph Isomorphism Network with edge features (primary model).
- **GATv2** [14]: Graph Attention Network v2 with edge features (generalization check).

The shared decoder applies global mean pooling over node embeddings, concatenates the 6-dimensional global feature vector \mathbf{g} , and passes the result through an MLP ($38 \rightarrow 16 \rightarrow 1$, where $38 = 32$ -dimensional graph embedding + 6 global features) with GELU activation and dropout ($p = 0.45$).

Self-supervised pretraining. Both encoders are pretrained via masked graph modeling on the 100,000 unlabeled corpus. We randomly mask 15% of nodes and 15% of edges independently per graph and train separate prediction heads to recover masked atom types (11-class cross-entropy) and masked bond types (5-class cross-entropy). Pretraining uses AdamW [24] ($\text{lr} = 5 \times 10^{-4}$, $\lambda = 10^{-4}$), batch size 64, cosine annealing LR, and early stopping with patience 10 over 65 epochs. The pretrained encoder weights are then transferred to the downstream model.

Fine-tuning. Downstream T_g prediction is trained with AdamW [24] ($\text{lr} = 5 \times 10^{-5}$, $\lambda = 3 \times 10^{-4}$) and ReduceLROnPlateau (factor 0.3, patience 30, $\text{lr}_{\text{min}} = 10^{-6}$). We use Huber loss with weighted sampling to balance the T_g distribution. Training runs for up to 85 epochs with early stopping (patience 30) after a minimum of 15 warm-up epochs. Batch size is 2 graphs; since each graph encodes an entire cup of polymer chains (tens to hundreds of chains, up to $\text{DP}_{\text{max}} = 1000$ repeat units per chain), the effective number of atoms per update step is large. Target T_g values are transformed to an approximately normal distribution using a quantile transformer and inverse-transformed before computing RMSE, so all reported errors are in Kelvin.

Evaluation protocol. We report test RMSE in Kelvin (K). Polymers are split using stratified 5-fold cross-validation, with folds balanced across three T_g strata: Low ($T_g < 250$ K), Mid ($250 \leq T_g < 400$ K), and High ($T_g \geq 400$ K). All cups of a given polymer are kept within the same fold to prevent data leakage. Cup-level predictions are averaged to produce one polymer-level prediction before computing RMSE. We repeat each experiment with 6 random seeds (30 runs total) and report mean \pm standard deviation. The same seeds and fold assignments are used for all compared methods. All experiments are run on a single NVIDIA A100-SXM4-40GB GPU. Graph construction for the labeled dataset takes 228 s in total (134 s for 201 copolymers, 94 s for 180 homopolymers). SSL corpus graph creation (100K trimers) takes 42 min; SSL encoder training is performed once and incurs a one-time computational cost. Fine-tuning (5-fold CV) takes approximately 128 min per seed, for a total of approximately 12.8 GPU-hours across all 30 runs. At inference, the SSL model predicts T_g for one polymer in $5.66 \text{ ms} \pm 0.80 \text{ ms}$ (mean \pm std over 5 folds, measured on the test set of approximately 75 polymers per fold).

7 Results

Pretraining unlocks the structural benefit. Table 1 summarizes test RMSE across all settings. Without SSL pretraining, the large-graph and repeat-unit constructions perform equivalently (28.40 K vs. 28.36 K, not significant), showing that a larger graph alone does not help when training from scratch on 381 labeled polymers. The structural richness of the Schulz-Zimm-sampled chains must first be learned through pretraining before it can be exploited at fine-tuning time.

With SSL pretraining, the picture changes substantially. Our large-graph construction achieves $24.76 \text{ K} \pm 3.30 \text{ K}$ across 30 evaluation runs (6 seeds \times 5 folds), compared to $26.08 \text{ K} \pm 4.20 \text{ K}$ for the repeat-unit baseline under the same protocol, a 5.1% reduction in mean error with strictly lower variance. A paired t -test on the 30 matched runs yields $t = 3.90$ ($p < 0.001$, $df = 29$), and the large-graph construction outperforms the repeat-unit baseline in 24 of 30 matched runs. The repeat-unit graph cannot encode chain-scale structure in its node embeddings regardless of how it is trained; SSL pretraining on diverse unlabeled chains gives the large-graph encoder the structural patterns it needs to exploit the molar mass distribution at inference time.

Architecture generalization. To verify that the benefit is not specific to GINE, we evaluate the same construction with a GATv2 [14] encoder. GATv2 achieves $24.73 \text{ K} \pm 2.75 \text{ K}$ (30 runs), nearly identical to GINE (24.76 K) and well below the repeat-unit baseline. Both models share identical graph construction, pretraining protocol, and decoder; only the message-passing mechanism differs. The consistent improvement across two architecturally distinct GNNs confirms that the gain originates from the graph construction and pretraining strategy, not from any architecture-specific inductive bias.

Table 1: Test RMSE (K) on the 381-polymer dataset. All results are mean \pm pooled std over 30 runs (6 seeds \times 5 folds). [†]Topology-only uses 1 seed, 5 folds. Lower is better.

Graph construction	Encoder	SSL	RMSE (K)
Topology-only (no chem. feats.) [†]	GINE	No	36.65 K \pm 4.38 K
Topology-only (no chem. feats.) [†]	GATv2	No	46.76 K \pm 2.04 K
Repeat-unit + global scalars	GINE	No	28.36 K \pm 4.53 K
Repeat-unit + global scalars	GATv2	No	28.47 K \pm 4.73 K
Large graph (ours) + globals	GINE	No	28.40 K \pm 4.34 K
Large graph (ours) + globals	GATv2	No	26.96 K \pm 4.15 K
Repeat-unit + global scalars	GINE	Yes	26.08 K \pm 4.20 K
Repeat-unit + global scalars	GATv2	Yes	25.52 K \pm 3.26 K
Large graph (ours) + globals	GINE	Yes	24.76 K \pm 3.30 K
Large graph (ours) + globals	GATv2	Yes	24.73 K \pm 2.75 K

Ablation: the role of chemical features. To isolate the contribution of atom and bond feature encoding, we evaluate a degenerate variant in which all node and edge features are replaced by constant all-ones vectors, retaining the Schulz-Zimm chain topology but stripping all chemical identity. This topology-only model achieves 36.65 K \pm 4.38 K (5 folds, 1 seed, base training). The 11.89 K gap relative to the full model is unambiguous: chain topology alone is far from sufficient, and rich chemical feature encoding is essential. Structural and chemical information are complementary: The topology determines which atoms interact across chain-scale distances, while atom and bond features determine what those interactions mean. We also ablate the number of independently sampled chains per polymer (cups) used during training and inference. Increasing cups from 1 to 3 reduces mean RMSE from 26.06 K to 24.48 K, a 6.1% improvement, as additional samples better cover the molar mass distribution. Beyond 3 cups the mean error plateaus; we select 4 cups as it recovers fold-to-fold variance relative to 3 cups (std: 3.30 K vs. 3.66 K) at no additional accuracy cost.

Uncertainty estimation. We apply Monte Carlo Dropout [15] to the SSL model with 30 stochastic forward passes per polymer (dropout active during inference). Each polymer receives a predictive mean T_g and sample standard deviation σ_{MC} as a proxy for epistemic uncertainty. Figure 3 shows predicted versus measured T_g values for all 381 polymers (out-of-fold predictions), with MC uncertainty as vertical error bars. Uncertainty is elevated at both tails of the T_g distribution: in the high- T_g regime ($T_g \geq 400$ K) and in the low- T_g regime ($T_g < 250$ K), both of which have fewer training examples than the mid- T_g stratum.

Summary. Table 1 summarizes all methods. Three findings are robust: (i) the large-graph construction unlocks significant improvement over repeat-unit graphs, but only in combination with SSL pretraining; (ii) chemical atom and bond features are indispensable alongside chain topology; (iii) the benefit is architecture-agnostic, holding for both GINE and GATv2 encoders.

8 Conclusion

We investigated the problem of graph construction for polymer property prediction, using glass transition temperature (T_g) as the target property. Standard practice represents a polymer by the graph of its repeat unit alone, discarding the chain-scale structure that governs T_g through chain entanglement and molar mass effects. Instead, we proposed to construct a large graph by sampling chains from the Schulz-Zimm molecular weight distribution parameterized by (M_n, M_w, \mathfrak{D}) , and to encode each atom and bond with rich chemical features via RDKit.

Our central empirical finding is that graph construction and self-supervised pretraining are jointly necessary given the scale of our labeled dataset. Without SSL, large graphs and repeat-unit graphs perform identically (28.40 K vs. 28.36 K), showing that the richer chain-scale topology offers no benefit when trained from scratch on only 381 labeled polymers. This likely reflects the limited scale of the labeled dataset rather than a fundamental limitation of the construction: a GNN trained on a few hundred samples cannot learn how chain-length patterns relate to the target property from supervision alone. With SSL pretraining on 100,000 unlabeled PSMILES, the encoder acquires a

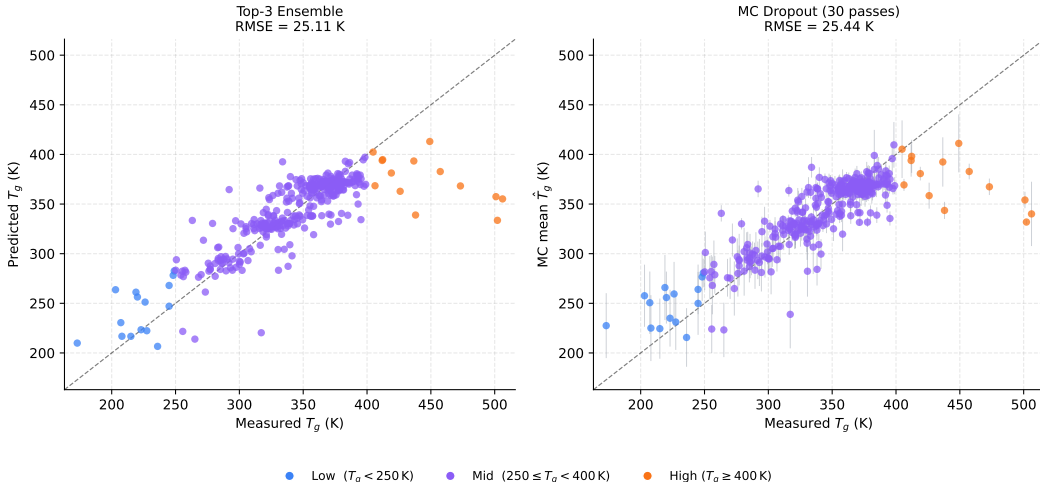


Figure 3: Predicted vs. measured T_g for all 381 polymers (out-of-fold predictions from one representative seed). **Left:** top-3 checkpoint ensemble predictions. **Right:** Monte Carlo Dropout mean with ± 1 std uncertainty bars (30 stochastic forward passes). Points are colored by T_g stratum: Low ($T_g < 250$ K, blue), Mid ($250 \leq T_g < 400$ K, purple), High ($T_g \geq 400$ K, orange).

chain-scale structural vocabulary before any T_g labels are seen, and the large-graph construction then achieves $24.76 \text{ K} \pm 3.30 \text{ K}$ RMSE, a statistically significant improvement over the repeat-unit baseline ($26.08 \text{ K} \pm 4.20 \text{ K}$, $p < 0.001$, paired t -test, 30 runs). Whether the large-graph construction would yield direct gains without SSL on substantially larger labeled datasets is an open question we were unable to answer with the data available, and is an important direction for future work.

An ablation stripping chemical features from the large graph degrades performance to 36.65 K, confirming that chain topology and chemical identity are both indispensable. The benefit is architecture-agnostic: GINE and GATv2 achieve nearly identical results (24.76 K and 24.73 K), making a model-specific explanation less likely.

Our construction may underperform in settings where multi-scale structure does not govern the target property, where the distributional descriptors (M_n , \mathfrak{D}) are unavailable or unreliable, or where the distribution is very narrow so that sampled chains are nearly identical.

Beyond the settings explored here, the full polymer-graph construction enables several capabilities over repeat-unit-only graphs that the present dataset does not yet exercise. First, end groups (the terminal chemical units that cap each chain) can be incorporated as additional nodes, which is especially consequential for low- M_n polymers where the end-group mass fraction is non-negligible; this representation also extends naturally to short biological macromolecules such as DNA, RNA, and proteins, where chain termini carry distinct chemistry. Second, branched, star, and hyperbranched polymer architectures are naturally encodable by varying the sampled chain topology, whereas repeat-unit graphs can only approximate such structures through ad hoc modifications. Third, tacticity (the stereochemical arrangement of side groups along the backbone, whether isotactic, syndiotactic, or atactic) is a sequence-level property requiring multiple consecutive repeat units to be present in the graph; once stereochemical sequence information is available in the input representation, for example through BigSMILES-style macromolecular notation [25], the full-chain representation can encode it without architectural changes, with relevance beyond T_g to crystallinity and phase behavior [26]. Fourth, copolymer microstructure, whether block (AAABBB) or random (ABABBA), is directly encodable as graph topology, allowing models to distinguish architectures that exhibit markedly different T_g signatures [27]; our current dataset contains only statistically random copolymers, making this a natural direction for future data collection and modeling.

These results suggest a broader principle: in data-scarce materials settings where the relevant structural descriptor is a distribution rather than a single canonical structure, encoding representative samples from that distribution directly into graph topology, combined with self-supervised pretraining on

unlabeled structural data, is a viable and effective strategy. Extending this to other polymer properties, other material classes, or larger labeled datasets remains an important direction for future work.

Acknowledgements

This work was funded by the European Research Council (ERC) under the European Union’s Horizon Europe programme (grant agreement No. 101220388, project genPI). The authors also thank the Federal Ministry for Economic Affairs and Energy (BMWE, project Digi-RoM, funding number: 03EE2072D) for financial support.

Usage of Generative AI

Generative AI was used solely for language editing (grammar, spelling, and clarity). It did not generate scientific content, perform calculations, or alter the authors’ interpretations, and all revisions were reviewed and approved by the authors.

Conflicts of Interest

The authors declare no conflicts of interest.

Data Availability

The datasets used in this study are described in Section 6. The code and model weights will be made publicly available in the Kuenneth Group GitHub repository (<https://github.com/kuennethgroup>) upon publication of this work.

References

- [1] Keith T. Butler, Daniel W. Davies, Hugh Cartwright, Olexandr Isayev, and Aron Walsh. Machine learning for molecular and materials science. *Nature*, 559:547–555, 2018. doi: 10.1038/s41586-018-0337-2.
- [2] Huan Tran, Rishi Gurnani, Chiho Kim, Ghanshyam Pilania, Ha-Kyung Kwon, Ryan P. Lively, and Rampi Ramprasad. Design of functional and sustainable polymers assisted by artificial intelligence. *Nature Reviews Materials*, aug 2024. doi: 10.1038/s41578-024-00708-8. URL <https://www.nature.com/articles/s41578-024-00708-8>.
- [3] Lihua Chen, Ghanshyam Pilania, Rohit Batra, Tran Doan Huan, Chiho Kim, Christopher Kuenneth, and Rampi Ramprasad. Polymer informatics: Current status and critical next steps. *Materials Science and Engineering: R: Reports*, 144:100595, 2021.
- [4] Lei Tao, Vikas Varshney, and Ying Li. Benchmarking machine learning models for polymer informatics: an example of glass transition temperature. *Journal of Chemical Information and Modeling*, 61(11):5395–5413, 2021.
- [5] Owen Queen, Gavin A McCarver, Saitheeraj Thatigotla, Brendan P Abolins, Cameron L Brown, Vasileios Maroulas, and Konstantinos D Vogiatzis. Polymer graph neural networks for multitask property learning. *npj Computational Materials*, 9(1):90, 2023.
- [6] Rishi Gurnani, Christopher Kuenneth, Aubrey Toland, and Rampi Ramprasad. Polymer informatics at scale with multitask graph neural networks. *Chemistry of Materials*, 35(4):1560–1567, 2023.
- [7] James E. Mark, Kia L. Ngai, William W. Graessley, Leo Mandelkern, Edward T. Samulski, Jack L. Koenig, and George D. Wignall. *Physical Properties of Polymers*. Cambridge University Press, 2004.

- [8] T. G. Fox and P. J. Flory. Second-order transition temperatures and related properties of polystyrene. i. influence of molecular weight. *Journal of Applied Physics*, 21(6):581–591, 1950. doi: 10.1063/1.1699711.
- [9] Michael Rubinstein and Ralph H. Colby. *Polymer Physics*. Oxford University Press, 2003.
- [10] Christopher Kuenneth and Rampi Ramprasad. polybert: a chemical language model to enable fully machine-driven ultrafast polymer informatics. *Nature Communications*, 14:4099, 2023.
- [11] David Weininger. Smiles, a chemical language and information system. 1. introduction to methodology and encoding rules. *Journal of Chemical Information and Computer Sciences*, 28(1):31–36, 1988.
- [12] Greg Landrum et al. RDKit: Open-source cheminformatics. <https://www.rdkit.org>, 2006.
- [13] Weihua Hu, Bowen Liu, Joseph Gomes, Marinka Zitnik, Percy Liang, Vijay Pande, and Jure Leskovec. Strategies for pre-training graph neural networks. In *International Conference on Learning Representations*, 2020.
- [14] Shaked Brody, Uri Alon, and Eran Yahav. How attentive are graph attention networks? In *International Conference on Learning Representations*, 2022.
- [15] Yarin Gal and Zoubin Ghahramani. Dropout as a Bayesian approximation: Representing model uncertainty in deep learning. In *Proceedings of the 33rd International Conference on Machine Learning*, volume 48, pages 1050–1059, 2016.
- [16] Justin Gilmer, Samuel S. Schoenholz, Patrick F. Riley, Oriol Vinyals, and George E. Dahl. Neural message passing for quantum chemistry. In *Proceedings of the 34th International Conference on Machine Learning*, pages 1263–1272, 2017.
- [17] Keyulu Xu, Weihua Hu, Jure Leskovec, and Stefanie Jegelka. How powerful are graph neural networks? In *International Conference on Learning Representations*, 2019.
- [18] Julian Kimmig, Yannik Köster, Timo Koswig, Punith Raviswamy, Subhash V. S. Ganti, Stefan Zechel, Christopher Kuenneth, and Ulrich S. Schubert. Structure-aware machine learning for polymers: A hierarchical graph network for predicting properties from statistical ensembles. *Macromolecular Rapid Communications*, 2026. doi: 10.1002/marc.202500671.
- [19] George Wypych. *Handbook of Polymers*. ChemTec Publishing, 2012.
- [20] J. Brandrup, E. H. Immergut, and E. A. Grulke, editors. *Polymer Handbook*. Wiley-Interscience, New York, 4 edition, 1999.
- [21] Zhuoying Jiang, Jiajie Hu, Babetta L. Marrone, Ghanshyam Pilania, and Xiong Yu. A deep neural network for accurate and robust prediction of the glass transition temperature of polyhydroxyalkanoate homo- and copolymers. *Materials*, 13(24):5701, 2020. doi: 10.3390/ma13245701.
- [22] Christopher Kuenneth and Rampi Ramprasad. polyone data set - 100 million hypothetical polymers including 29 properties. Zenodo, 2022.
- [23] Tianle Cai, Shengjie Luo, Keyulu Xu, Di He, Tie-Yan Liu, and Liwei Wang. GraphNorm: A principled approach to accelerating graph neural network training. In *Proceedings of the 38th International Conference on Machine Learning*, 2021.
- [24] Ilya Loshchilov and Frank Hutter. Decoupled weight decay regularization. In *International Conference on Learning Representations*, 2019.
- [25] Tzyy-Shyang Lin, Connor W. Coley, Hidenobu Mochigase, Haley K. Beech, Wencong Wang, Zi Wang, Eliot Woods, Stephen L. Craig, Jeremiah A. Johnson, Julia A. Kalow, Klavs F. Jensen, and Bradley D. Olsen. BigSMILES: A structurally-based line notation for describing macromolecules. *ACS Central Science*, 5(9):1523–1531, 2019. doi: 10.1021/acscentsci.9b00476.

- [26] Ling Chang and E. M. Woo. Tacticity effects on glass transition and phase behavior in binary blends of poly(methyl methacrylate)s of three different configurations. *Polymer Chemistry*, 1: 198–202, 2010. doi: 10.1039/B9PY00237E.
- [27] Jungki Kim, Michelle M. Mok, Robert W. Sandoval, Dong Jin Woo, and John M. Torkelson. Uniquely broad glass transition temperatures of gradient copolymers relative to random and block copolymers containing repulsive comonomers. *Macromolecules*, 39(18):6152–6160, 2006. doi: 10.1021/ma061241f.

9 Appendix

Model Sensitivity Analysis: What the GNN Learns About Dispersity and Chain Length

A natural question is whether the model has merely learned a simple monotonic rule (e.g., “higher \mathfrak{D} always raises T_g by a fixed amount”) or whether it has internalized a more physically nuanced relationship between the molecular weight distribution and the T_g . To probe this, we construct a controlled sweep: for five homopolymers selected from the training distribution, we generate a 10×10 grid spanning $M_n \in [2,000, 20,000]$ and $\mathfrak{D} \in [1.5, 4.0]$, giving 500 synthetic entries with no observed T_g . We run inference with a single trained fold checkpoint and compute the finite-difference sensitivity $\partial \hat{T}_g / \partial \mathfrak{D}$ at each grid point. We highlight two contrasting polymers in Figures 4 and 5.

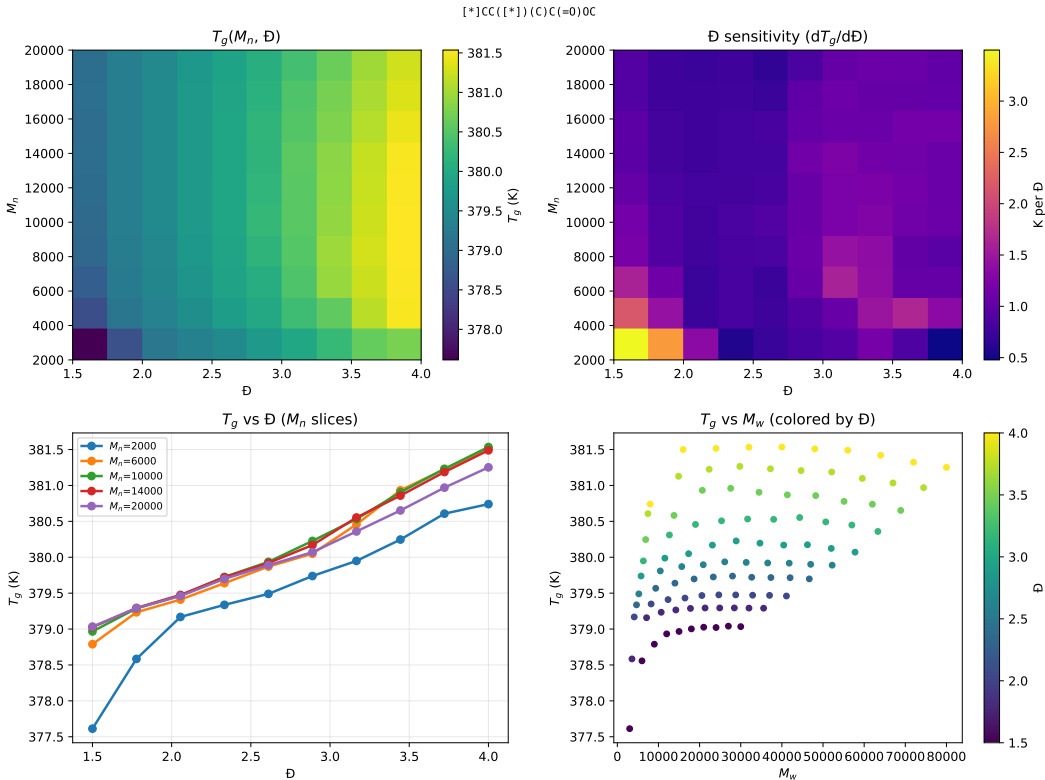


Figure 4: Sensitivity sweep for PSMILES [*]CC([*])(C)C(=O)OC. Note the crossing M_n slices at low \mathfrak{D} (bottom-left): higher M_n yields lower \hat{T}_g in the low-dispersity regime, a non-monotonic interaction invisible to additive models. Sensitivity magnitude is low throughout (< 3 K per \mathfrak{D} unit) with a patchy, non-uniform spatial structure.

Non-linearity and saturation. The bottom-left panels show \hat{T}_g as a function of \mathfrak{D} at fixed M_n slices. In both polymers the response is concave: the largest gains in \hat{T}_g occur at low \mathfrak{D} , and the curve flattens as \mathfrak{D} increases. A linear model would produce parallel straight lines with equal slope everywhere; the model instead predicts diminishing returns, consistent with the physical intuition that once the molecular weight distribution is broad enough, further polydispersity has a progressively smaller effect on chain entanglement and hence on T_g .

M_n - \mathfrak{D} interaction and polymer-specific magnitude. The sensitivity heatmaps (top-right panels) reveal that $\partial \hat{T}_g / \partial \mathfrak{D}$ is not constant across the (M_n, \mathfrak{D}) plane. For the polymer in Figure 5, sensitivity reaches up to ~ 30 K per \mathfrak{D} unit, an order of magnitude larger than for the polymer in Figure 4 (< 3 K per \mathfrak{D} unit throughout). This contrast shows the model has learned chemistry-dependent sensitivity rather than a universal shift applied uniformly to all repeat units.

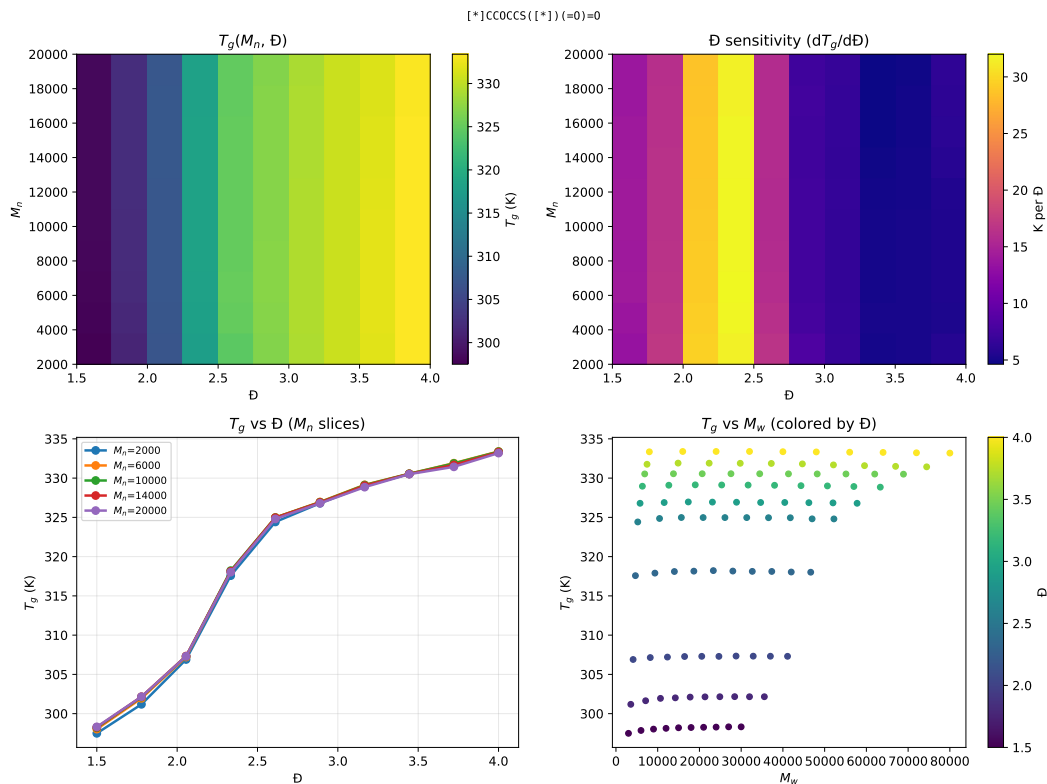


Figure 5: Sensitivity sweep for PSMILES $[*]CCOCCS([*])(=O)=O$. \hat{T}_g spans ~ 37 K across the grid and sensitivity reaches up to 30 K per \mathcal{D} unit at low \mathcal{D} , an order of magnitude larger than in Figure 4. The concave \hat{T}_g - \mathcal{D} curves (bottom-left) show diminishing returns as \mathcal{D} increases.

Non-monotonic M_n effect. In Figure 4, the M_n slices in the line plot cross at low \mathcal{D} : higher M_n yields a lower predicted T_g in that regime. This non-monotonic interaction, which would be invisible to any model that treats M_n and \mathcal{D} as independent additive inputs, suggests the GNN has captured a coupling between chain stiffness, steric bulk, and chain-length effects that produces qualitatively different behavior depending on the dispersity regime.

Taken together, these results indicate that the model has not collapsed to a simple linear or separable function of the molecular weight descriptors. The graph-based representation combined with global descriptor conditioning allows the model to express interactions between local chemistry and chain-scale statistics that are consistent with polymer chemistry.

Atom and Bond Feature Encoding

Tables 2 and 3 list all features used to construct the node feature matrix $\mathbf{X} \in \mathbb{R}^{|\mathcal{V}| \times 31}$ and edge feature matrix $\mathbf{E} \in \mathbb{R}^{|\mathcal{E}| \times 14}$. All features are computed with RDKit [12]. One-hot vectors append an “other” bin for out-of-vocabulary values.

Table 2: Atom (node) features. Total dimension $d_v = 31$.

Feature	Encoding	Dim
Atom type	One-hot: [* , B, C, N, O, F, P, S, Cl, Br, I, other]	12
Hybridization	One-hot: [SP, SP ² , SP ³ , other]	4
Chirality	One-hot: [CW, CCW, unspecified]	3
Degree	One-hot: [0, 1, 2, 3, 4, 5, other]	7
Is aromatic	Binary scalar	1
Is in ring	Binary scalar	1
Total # of Hs	Integer scalar	1
Formal charge	Integer scalar	1
Atomic mass	Scalar (divided by 100)	1
Total		31

Table 3: Bond (edge) features. Total dimension $d_e = 14$.

Feature	Encoding	Dim
Bond type	One-hot: [single, double, triple, aromatic, other]	5
Stereo	One-hot: [none, Z, E, cis, trans, any, other]	7
Is conjugated	Binary scalar	1
Is in ring	Binary scalar	1
Total		14